Journal of Sound and Vibration (2001) **240**(4), 733–746
doi:10.1006/jsvi.2000.3241, available online at http://www.idealibrary.com on IDEAL®

VIBRATION OF AN AXIALLY MOVING STRING WITH GEOMETRIC NON-LINEARITY AND TRANSLATING ACCELERATION

J. CHUNG AND C. S. HAN

Department of Mechanical Engineering, Hanyang University, 1271 *Sa*-1-*dong*, *Ansan*, *Kyunggi-do* 425-791, *Republic of Korea. E-mail*: *jchung@email.hanyang.ac.kr*

AND

K. YI

School of Mechanical Engineering, Hanyang University, 17 *Haengdang-dong*, *Seongdong-ku*, *Seoul* 133-791, *Republic of Korea*

(*Received* 19 *May* 2000, *and in final form* 4 *August* 2000)

The vibration of an axially moving string is studied when the string has geometric non-linearity and translating acceleration. Based upon the von Karman strain theory, the equations of motion are derived considering the longitudinal and transverse deflections. The equation for the longitudinal vibration is linear and uncoupled, while the equation for the transverse vibration is non-linear and coupled between the longitudinal and transverse deflections. These equations are discretized by the Galerkin method after they are transformed into the variational equations, i.e., the weak forms so that the admissible and comparison functions can be used for the bases of the longitudinal and transverse deflections respectively. With the discretized equations, the natural frequencies, the time histories of the deflections, and the distributions of the deflection and stress are investigated. In addition, comparisons between the results of linear and non-linear theories are provided.

1. INTRODUCTION

Transverse vibrations of an axially moving string have been investigated by many researchers, because a variety of physical systems may be modelled as axially moving strings, e.g., belts, tapes, paper and fibres. Comprehensive reviews on the dynamics of axially moving strings are given in references [1, 2]. Most of the analyses for the vibration and stability of axially moving strings have mainly focused on the transverse deflection. Qualitative and quantitative studies for the non-linear vibrations of axially moving strings were performed by Mote [3] and Thurman and Mote [4]. In their studies, the non-linear strain was derived considering the geometric non-linearity and the infinitesimal strain simultaneously. However, it is reasonable that the geometric non-linearity is considered in the general Lagrangian strain that is often called the von Karman strain, because the infinitesimal strain theory is suitable for a linear system while the von Karman strain theory is for a non-linear system [5]. On the other hand, many authors presented studies on the vibration and stability of axially moving strings when the strings had axial acceleration [6–9].

0022-460X/01/090733 + 14 $35.00/0

In this study, the equations of motion for an axially moving string are derived from the extended Hamilton principle [10], when the string has transverse and longitudinal deflections, geometric non-linearity and translating acceleration. The geometric non-linear characteristics are considered by adopting the von Karman strain theory instead of the approximated infinitesimal strain theory. The weak forms or the variational equations corresponding to the equations of motion are discretized by the Galerkin method, in which the admissible and comparison functions are used as basis functions for the longitudinal and transverse deflections respectively. Based on the discretized equations, to investigate the dynamic behaviours of the string, the natural frequencies and the dynamic responses are obtained for the longitudinal and transverse vibrations. The time histories and distributions for the deflections and the stress are computed by the generalized-α method [11]. Additionally, computation results from the non-linear theory are compared with those from the linear theory.

2. THEORETICAL MODEL AND EQUATIONS OF MOTION

Figure 1(a) shows a string drive system, containing driving and driven pulleys which have the same radius R and the same mass moment of inertia J. The driving pulley is subjected to a torque $M_T(t)$. The string has the mass density per length ρ, the cross-sectional area A, Young's modulus E, the translating speed $V(t)$ and the acceleration $\dot{V}(t)$. A model of the axially moving string with the transverse load per length $p(x, t)$ is shown in Figure 1(b), where two supports are separated by a distance L and the longitudinal and transverse deflections are represented by $u(x, t)$ and $v(x, t)$ respectively. Assuming that there exists no friction in the axes of the pulleys, the acceleration may be expressed as

$$\dot{V}(t) = \frac{R}{2(J + \rho L R^2)} M_T(t). \tag{1}$$

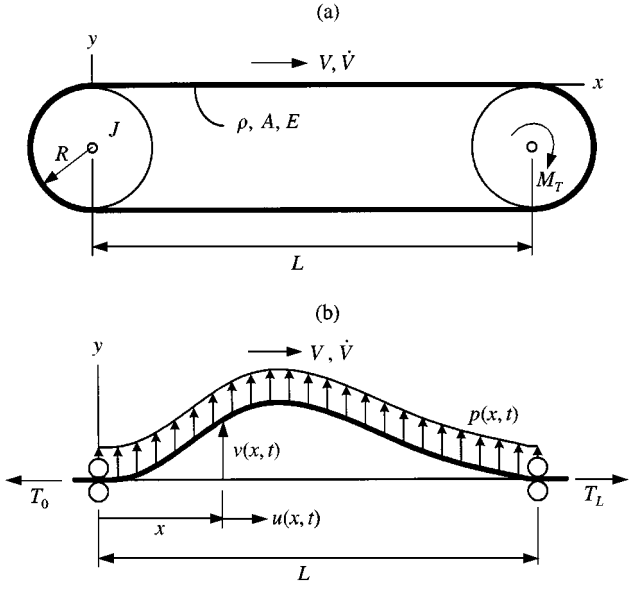

Figure 1. Schematics of an axially moving string: (a) a string drive system between two pulleys; and (b) a theoretical model of the string with the longitudinal and transverse deflections.

If the initial tension is T_0 when $M_T = 0$ and the tension at $x = L$ is T_L when $M_T \neq 0$, the relation between T_0 and T_L is given by

$$T_L = T_0 + \rho L \dot{V} \tag{2}$$

The equations of motion are derived by using the extended Hamilton principle [10], because mass is transported across the boundaries of $x = 0$ and L. In this case, Hamilton's principle is expressed as

$$\int_{t_1}^{t_2} (\delta T - \delta U + \delta W_{nc} - \delta M)\, \mathrm{d}t = 0, \tag{3}$$

where t_1 and t_2 are any two instants, T the kinetic energy, U the potential energy, δW_{nc} the virtual work done by the non-conservative forces, and δM the virtual momentum transport across the boundaries. After the string is deformed, the position vector of a point at x can be written as

$$\mathbf{r} = (x + u)\mathbf{i} + v\mathbf{j}, \tag{4}$$

where $\mathbf{i}$ and $\mathbf{j}$ are the unit vectors along the x- and y-axes respectively. The material derivative of $\mathbf{r}$ yields the velocity vector

$$\mathbf{v} = \left(V + \frac{\partial u}{\partial t} + V\frac{\partial u}{\partial x}\right)\mathbf{i} + \left(\frac{\partial v}{\partial t} + V\frac{\partial v}{\partial x}\right)\mathbf{j}. \tag{5}$$

On the other hand, when the geometric non-linearity is considered for the elastic string, the displacement–strain relation [12] and the strain–stress relation are given by

$$\varepsilon_x = \frac{\partial u}{\partial x} + \frac{1}{2}\left(\frac{\partial v}{\partial x}\right)^2, \qquad \sigma_x = E\varepsilon_x. \tag{6}$$

Neglecting the gravity, the kinetic and potential energies are computed by

$$T = \frac{1}{2}\rho \int_0^L \mathbf{v}\cdot\mathbf{v}\, \mathrm{d}x, \qquad U = \frac{1}{2}A\int_0^L \sigma_x \varepsilon_x\, \mathrm{d}x. \tag{7}$$

and the virtual work done by the non-conservative forces and the virtual momentum transport are expressed as

$$\delta W_{nc} = -T_0\, \delta u|_{x=0} + T_L\, \delta u|_{x=L} + \int_0^L p(x,t)\, \delta v\, \mathrm{d}x, \qquad \delta M = \rho(\mathbf{v}\cdot\delta\mathbf{r})(V\ \mathbf{i}\cdot\mathbf{n})|_{x=0}^{L}, \tag{8}$$

where $\mathbf{n}$ is the outward normal vector at the boundaries. The equations of motion can be obtained by substituting equations (7) and (8) into equation (3).

Governing equations of motion for the axially moving string with the longitudinal and transverse deflections are given by

$$\rho\left(\frac{\partial^2 u}{\partial t^2} + 2V\frac{\partial^2 u}{\partial t\,\partial x} + V^2\frac{\partial^2 u}{\partial x^2} + \dot{V}\frac{\partial u}{\partial x}\right) - EA\frac{\partial^2 u}{\partial x^2} = -\rho\dot{V}, \tag{9}$$

$$\rho\left(\frac{\partial^2 v}{\partial t^2} + 2V\frac{\partial^2 v}{\partial t\,\partial x} + V^2\frac{\partial^2 v}{\partial x^2} + \dot{V}\frac{\partial v}{\partial x}\right) - EA\frac{\partial}{\partial x}\left(\frac{\partial u}{\partial x}\frac{\partial v}{\partial x}\right) = p \tag{10}$$

and the boundary conditions are given by

$$EA\frac{\partial u}{\partial x} = T_0 \quad \text{at } x = 0, \quad EA\frac{\partial u}{\partial x} = T_0 + \rho L\dot{V} \quad \text{at } x = L, \quad v = 0 \quad \text{at } x = 0, L. \tag{11}$$

Introducing the dimensionless variables

$$\tau = \frac{\sqrt{EA/\rho}}{L}t, \quad \xi = \frac{x}{L}, \quad \phi = \frac{u}{L}, \quad \psi = \frac{v}{L}, \quad c = \frac{V}{\sqrt{EA/\rho}}, \quad \dot{c} = \frac{\rho L\dot{V}}{EA}, \quad h = \frac{T_0}{EA}, \quad \gamma = \frac{p}{EA/L} \tag{12}$$

into equations (9) and (10) yields the dimensionless equations of motion

$$\frac{\partial^2\phi}{\partial\tau^2} + 2c\frac{\partial^2\phi}{\partial\tau\partial\xi} - (1 - c^2)\frac{\partial^2\phi}{\partial\xi^2} + \dot{c}\frac{\partial\phi}{\partial\xi} = -\dot{c}, \tag{13}$$

$$\frac{\partial^2\psi}{\partial\tau^2} + 2c\frac{\partial^2\psi}{\partial\tau\,\partial\xi} + c^2\frac{\partial^2\psi}{\partial\xi^2} - \frac{\partial}{\partial\xi}\left(\frac{\partial\phi}{\partial\xi}\frac{\partial\psi}{\partial\xi}\right) + \dot{c}\frac{\partial\psi}{\partial\xi} = \gamma. \tag{14}$$

The boundary conditions corresponding to equations (11) are

$$\frac{\partial\phi}{\partial\xi} = h \quad \text{at } \xi = 0, \quad \frac{\partial\phi}{\partial\xi} = h + \dot{c} \quad \text{at } \xi = 1, \quad \psi = 0 \quad \text{at } \xi = 0, 1. \tag{15}$$

If the translating velocity is constant and the tension is uniform along the string, the equations of motion and the associated boundary conditions reduce to

$$\frac{\partial\phi}{\partial\xi} = h = \text{const}, \tag{16}$$

$$\frac{\partial^2\psi}{\partial\tau^2} + 2c\frac{\partial^2\psi}{\partial\tau\,\partial\xi} - (h - c^2)\frac{\partial^2\psi}{\partial\xi^2} = \gamma, \tag{17}$$

$$\psi = 0 \quad \text{at } \xi = 0, 1. \tag{18}$$

Note that equation (17) is the well-known equation of motion for an axially moving string with a constant translating speed and a uniform tension.

3. DISCRETIZATION OF THE EQUATIONS OF MOTION

In order to obtain approximate solutions in a finite-dimensional function space, the Galerkin method is applied to the variational equations, i.e., the weak forms [13] that are derived from equations (13) and (14) with the boundary conditions (15). Denoting by $\bar{\phi}$ and $\bar{\psi}$ the weighting functions corresponding to the trial functions ϕ and ψ, respectively, the

weak forms of equations (13) and (14) may be expressed as

$$\int_0^1 \left[\bar{\phi} \frac{\partial^2 \phi}{\partial \tau^2} + c\left(\bar{\phi} \frac{\partial^2 \phi}{\partial \tau \, \partial \xi} - \frac{\partial \bar{\phi}}{\partial \xi} \frac{\partial \phi}{\partial \tau} \right) + (1 - c^2) \frac{\partial \bar{\phi}}{\partial \xi} \frac{\partial \phi}{\partial \xi} + \frac{\dot{c}}{2} \left(\bar{\phi} \frac{\partial \phi}{\partial \xi} - \frac{\partial \bar{\phi}}{\partial \xi} \phi \right) \right] \mathrm{d}\xi$$

$$= -c \left[\bar{\phi} \frac{\partial \phi}{\partial \tau} \right]_{\xi=0}^{1} + (1 - c^2) \left[(h + \dot{c}) \bar{\phi}(1) - h \bar{\phi}(0) \right] - \frac{\dot{c}}{2} [\bar{\phi}\phi]_{\xi=0}^{1} - \dot{c} \int_0^1 \bar{\phi} \, \mathrm{d}\xi, \quad (19)$$

$$\int_0^1 \left[\bar{\psi} \frac{\partial^2 \psi}{\partial \tau^2} + c\left(\bar{\psi} \frac{\partial^2 \psi}{\partial \tau \, \partial \xi} - \frac{\partial \bar{\psi}}{\partial \xi} \frac{\partial \psi}{\partial \tau} \right) + \frac{\partial \bar{\psi}}{\partial \xi} \left(\frac{\partial \phi}{\partial \xi} \frac{\partial \psi}{\partial \xi} - c^2 \frac{\partial \psi}{\partial \xi} \right) + \frac{\dot{c}}{2} \left(\bar{\psi} \frac{\partial \psi}{\partial \xi} - \frac{\partial \bar{\psi}}{\partial \xi} \psi \right) \right] \mathrm{d}\xi$$

$$= \int_0^1 \bar{\psi} \gamma \, \mathrm{d}\xi. \quad (20)$$

It is noted that the longitudinal deflection may be approximated as a series of the admissible functions while the transverse deflection should be approximated as a series of the comparison functions, because the natural boundary conditions for ϕ have been already considered in the weak form given by equation (19). Therefore, the dimensionless longitudinal and transverse deflections are approximated by the trial functions that are linear combinations of the admissible and comparison functions, respectively,

$$\phi(\xi, \tau) = \sum_{j=1}^{J} C_j(\tau) \cos j\pi\xi, \qquad \psi(\xi, \tau) = \sum_{n=1}^{N} S_n(\tau) \sin n\pi\xi \quad (21)$$

and in a similar manner the weighting functions corresponding to the trial functions are approximated by

$$\bar{\phi}(\xi, \tau) = \sum_{i=1}^{J} \bar{C}_i(\tau) \cos i\pi\xi, \qquad \bar{\psi}(\xi, \tau) = \sum_{m=1}^{N} \bar{S}_m(\tau) \sin m\pi\xi, \quad (22)$$

where J and N are the total numbers of the basis functions for the longitudinal and transverse deflections, respectively, $C_j(\tau)$ and $S_n(\tau)$ are unknown functions of τ to be determined, and $\bar{C}_i(\tau)$ and $\bar{S}_m(\tau)$ are arbitrary functions of τ.

The Galerkin method is used to obtain the discretized equations of motion from the weak forms. When collecting all the terms of equations (19) and (20) with respect to $\bar{C}_i(\tau)$ and $\bar{S}_m(\tau)$ after substituting equations (21) and (22) into equations (19) and (20), the coefficients of $\bar{C}_i(\tau)$ and $\bar{S}_m(\tau)$ provide the discretized equations given by

$$\sum_{j=0}^{J} [m_{ij}^c \ddot{C}_j + 2c g_{ij}^c \dot{C}_j + (1 - c^2) k_{ij}^c C_j + \dot{c} g_{ij}^c C_j] = f_i^c, \; i = 1, 2, \ldots, J, \quad (23)$$

$$\sum_{n=1}^{N} \left\{ m_{mn}^s \ddot{S}_n + 2c g_{mn}^s \dot{S}_n + \left[\sum_{i=1}^{J} \alpha_{imn} C_i - c^2 k_{mn}^s \right] S_n + \dot{c} g_{mn}^s S_n \right\} = f_m^s, \; m = 1, 2, \ldots, N, \quad (24)$$

where the superposed dots indicate derivatives with respect to the dimensionless time τ and

$$m^c_{ij} = \tfrac{1}{2}\delta_{ij}, \qquad m^s_{mn} = \tfrac{1}{2}\delta_{mn},$$

$$g^c_{ij} = \begin{cases} 0, & \text{for } i = j, \\ \dfrac{1-(-1)^{i+j}}{2}\dfrac{i^2+j^2}{i^2-j^2} & \text{for } i \neq j, \end{cases} \qquad g^s_{mn} = \begin{cases} 0, & \text{for } m = n, \\ [1-(-1)^{m+n}]\dfrac{mn}{m^2-n^2} & \text{for } m \neq n, \end{cases}$$

$$k^c_{ij} = \frac{i^2\pi^2}{2}\delta_{ij}, \qquad k^s_{mn} = \frac{m^2\pi^2}{2}\delta_{mn},$$

$$\alpha_{imn} = \begin{cases} -\dfrac{2i^2 mn(i^2-m^2-n^2)\pi^2}{(i+m+n)(i+m-n)(i-m+n)(i-m-n)} & \text{if } i+m+n \text{ is odd}, \\ 0 & \text{if } i+m+n \text{ is even}, \end{cases}$$

$$f^c_i = (1-c^2)\,[(h+\dot{c})(-1)^i - h], \qquad f^s_m = \int_0^1 \gamma \sin m\pi\xi d\xi, \tag{25}$$

in which δ_{ij} and δ_{mn} are the Kronecker delta functions. Equations (23) and (24) can be written in matrix-vector form:

$$\mathbf{M}_c\ddot{\mathbf{C}} + 2c\mathbf{G}_c\dot{\mathbf{C}} + [(1-c^2)\mathbf{K}_c + \dot{c}\mathbf{G}_c]\mathbf{C} = \mathbf{F}_c, \tag{26}$$

$$\mathbf{M}_s\ddot{\mathbf{S}} + 2c\mathbf{G}_s\dot{\mathbf{S}} + [\mathbf{K}_{sc}(\mathbf{C}) - c^2\mathbf{K}_s + \dot{c}\mathbf{G}_s]\mathbf{S} = \mathbf{F}_s, \tag{27}$$

where

$$\mathbf{C} = \{C_1, C_2, \ldots, C_J\}^{\mathrm{T}}, \qquad \mathbf{S} = \{S_1, S_2, \ldots, S_N\}^{\mathrm{T}}, \quad \mathbf{K}_{sc}(\mathbf{C}) = \left[\sum_{i=1}^{J} \alpha_{imn} C_i\right]. \tag{28}$$

Note that equation (26) is a linear ordinary differential equation while equation (27) is a non-linear ordinary differential equation. Furthermore, the longitudinal deflection is coupled with the transverse deflection in equation (27). This means that the longitudinal vibration has an influence on the transverse vibration.

4. NATURAL FREQUENCIES

Consider the convergence characteristics of the natural frequencies for the axially moving string when the translating speed is constant and the applied transverse force is zero. In order to compute the natural frequencies, the linear equations of motion should be derived from equations (26) and (27). Denoting the equilibrium solutions of equations (26) and (27) by $\mathbf{C}^*$ and $\mathbf{S}^*$ respectively, the elements of $\mathbf{C}^*$ and $\mathbf{S}^*$ can be expressed as

$$C^*_i = \frac{2h[(-1)^i - 1]}{\pi^2 i^2}, \qquad S^*_m = 0. \tag{29}$$

Even though an analytical verification cannot be provided in this paper, it can be numerically verified that $\mathbf{K}_{sc}(\mathbf{C}^*)$ approaches $h\mathbf{K}_s$ as the numbers of the basis functions, J and N, increase. Using this fact, the linearization of equations (26) and (27) in the

TABLE 1

Convergence characteristics of the dimensionless natural frequencies λ for the longitudinal vibration when $c = 0{\cdot}35$ and $h = 0{\cdot}25$

J	λ_1	λ_2	λ_3	λ_4
1	2·9429	N/A	N/A	N/A
2	2·6881	6·4437	N/A	N/A
3	2·6772	5·7058	10·0109	N/A
4	2·6608	5·5350	8·8800	13·7644
5	2·6588	5·5294	8·3972	12·1754
6	2·6525	5·5026	8·3818	11·2652
7	2·6517	5·5001	8·3395	11·1298
8	2·6484	5·4889	8·3363	11·1043
9	2·6479	5·4874	8·3195	11·0787
10	2·6458	5·4813	8·3183	11·0685
11	2·6455	5·4802	8·3089	11·0580
12	2·6441	5·4763	8·3083	11·0522
13	2·6439	5·4755	8·3022	11·0465
14	2·6429	5·4728	8·3019	11·0427
15	2·6427	5·4722	8·2976	11·0391
16	2·6419	5·4701	8·2974	11·0364
17	2·6418	5·4697	8·2942	11·0339
18	2·6412	5·4681	8·2941	11·0318
19	2·6411	5·4677	8·2916	11·0300
20	2·6406	5·4665	8·2915	11·0284

neighbourhood of the equilibrium solutions leads to

$$\mathbf{M}_c\ddot{\mathbf{C}} + 2c\mathbf{G}_c\dot{\mathbf{C}} + (1 - c^2)\mathbf{K}_c\mathbf{C} = \mathbf{0}, \tag{30}$$

$$\mathbf{M}_s\ddot{\mathbf{S}} + 2c\mathbf{G}_s\dot{\mathbf{S}} + (h - c^2)\mathbf{K}_s\mathbf{S} = \mathbf{0}, \tag{31}$$

from which the natural frequencies can be computed for the longitudinal and transverse vibrations. Denote the dimensionless natural frequency for the natural frequency ω by

$$\lambda = \frac{\omega}{\sqrt{EA/\rho L^2}}. \tag{32}$$

Tables 1 and 2 demonstrate that the dimensionless natural frequencies for the longitudinal and transverse vibrations are converged with J and N when $c = 0{\cdot}35$ and $h = 0{\cdot}25$. As shown in Tables 1 and 2, it is reasonable that $J = N = 20$ are chosen in further computations.

The effects of the translating speed and the longitudinal load on the natural frequencies are analyzed for both the longitudinal and transverse vibrations. Figure 2 describes the variation of the lowest four dimensionless natural frequencies λ for the dimensionless speed c, when the dimensionless longitudinal load has a constant value of $h = 0{\cdot}25$. As shown in Figure 2, the critical speed is $c = 1$ for the longitudinal vibration and $c = 0{\cdot}5$ for the transverse vibrations. These results are compatible with equations (30) and (31) which imply that the critical speeds are $c = 1$ and $\sqrt{h}$ for the longitudinal and transverse vibrations

TABLE 2

Convergence characteristics of the dimensionless natural frequencies λ for the transverse vibration when $c = 0{\cdot}35$ and $h = 0{\cdot}25$

N	λ_1	λ_2	λ_3	λ_4
1	1·1218	N/A	N/A	N/A
2	0·8353	3·0131	N/A	N/A
3	0·8050	1·9970	5·2683	N/A
4	0·8044	1·6471	3·7421	7·6655
5	0·8022	1·6161	2·7627	5·8731
6	0·8021	1·6107	2·4433	4·3902
7	0·8015	1·6069	2·4290	3·4876
8	0·8015	1·6055	2·4154	3·2414
9	0·8013	1·6044	2·4131	3·2398
10	0·8013	1·6038	2·4089	3·2195
11	0·8012	1·6034	2·4083	3·2194
12	0·8012	1·6031	2·4064	3·2124
13	0·8012	1·6029	2·4062	3·2124
14	0·8012	1·6028	2·4053	3·2093
15	0·8012	1·6027	2·4051	3·2093
16	0·8012	1·6026	2·4046	3·2076
17	0·8011	1·6025	2·4045	3·2076
18	0·8011	1·6025	2·4042	3·2066
19	0·8011	1·6024	2·4042	3·2066
20	0·8011	1·6024	2·4040	3·2060

respectively. Since the real parts of the eigenvalues are positive for the speed above the critical speeds, in other words, the system is dynamically unstable, the dimensionless natural frequencies in the regions above the critical speeds are not plotted in Figure 2. On the other hand, the effects of the dimensionless longitudinal load h on the dimensionless natural frequencies λ are presented in Figure 3, where the dimensionless translating speed c is fixed at a constant value of 0·35. Figure 3 shows that the natural frequencies for the longitudinal vibration are independent of h while the frequencies for the transverse vibration are dependent on h. Similarly, with Figure 2(b), Figure 3(b) does not describe the behaviour of the natural frequencies in the region of $h < c^2$ (in this case, $h < 0{\cdot}1125$), because the string becomes unstable.

5. DYNAMIC RESPONSES

The time histories of the deflections as well as the distributions of the deflections and the stress may be obtained from equations (26) and (27) by using the generalized-α method [11]. To apply the generalized-α method to the equations, it is convenient to express the discretized equation (26) as

$$\mathbf{M}_c \mathbf{a}^c_{n+1-\alpha_m} + 2c\mathbf{G}_c \mathbf{v}^c_{n+1-\alpha_f} + [(1-c^2)\mathbf{K}_c + \dot{c}\mathbf{G}_c]\mathbf{d}^c_{n+1-\alpha_f} = \mathbf{F}^c_{n+1-\alpha_f}, \tag{33}$$

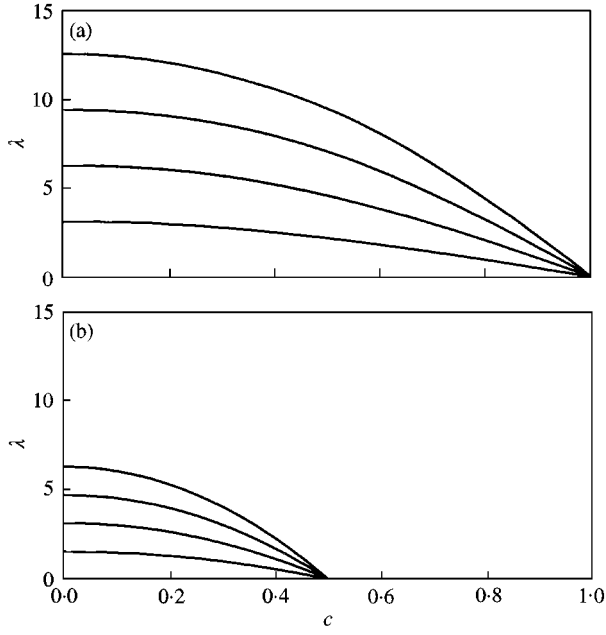

Figure 2. Dimensionless natural frequencies λ versus the dimensionless translating speed c when $h = 0{\cdot}25$: (a) the longitudinal vibration; and (b) the transverse vibration.

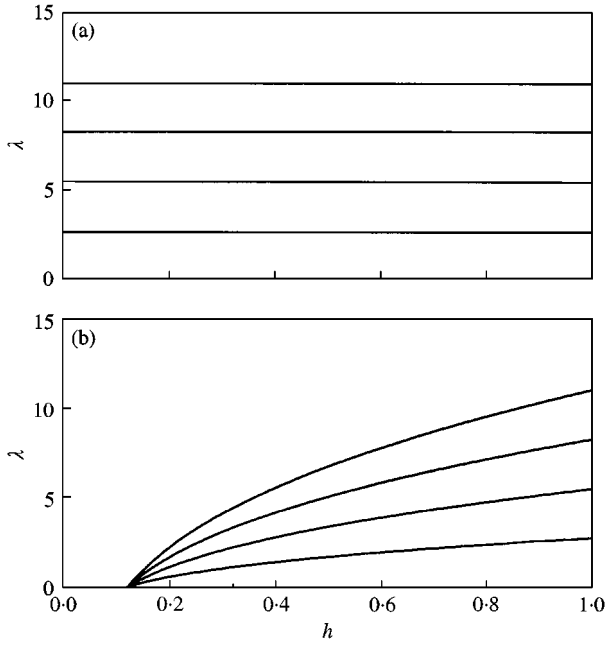

Figure 3. Dimensionless natural frequencies λ versus the dimensionless longitudinal load h when $c = 0{\cdot}35$: (a) the longitudinal vibration; and (b) the transverse vibration.

where

$$\mathbf{d}^c_{n+1-\alpha_f} = (1-\alpha_f)\,\mathbf{d}^c_{n+1} + \alpha_f\,\mathbf{d}^c_n, \qquad \mathbf{v}^c_{n+1-\alpha_f} = (1-\alpha_f)\,\mathbf{v}^c_{n+1} + \alpha_f\,\mathbf{v}^c_n,$$

$$\mathbf{a}^c_{n+1-\alpha_m} = (1-\alpha_m)\,\mathbf{a}^c_{n+1} + \alpha_m\,\mathbf{a}^c_n, \qquad \mathbf{F}^c_{n+1-\alpha_f} = \mathbf{F}_c((1-\alpha_f)\,\tau_{n+1} + \alpha_f\,\tau_n), \tag{34}$$

$$\mathbf{d}^c_{n+1} = \mathbf{d}^c_n + \Delta\tau\mathbf{v}^c_n + (\tfrac{1}{2}-\beta)\,\Delta\tau^2\mathbf{a}^c_n + \beta\Delta\tau^2\mathbf{a}^c_{n+1}, \qquad \mathbf{v}^c_{n+1} = \mathbf{v}^c_n + (1-\gamma)\,\Delta\tau\mathbf{a}^c_n + \gamma\Delta\tau\mathbf{a}^c_{n+1}, \tag{35}$$

in which α_m, α_f, β and γ are the algorithmic parameters determined by the numerical dissipation parameter; $\Delta\tau$ is the time step size, i.e., $\Delta\tau = \tau_{n+1} - \tau_n$; $\mathbf{d}^c_n$, $\mathbf{v}^c_n$ and $\mathbf{a}^c_n$ are approximations to $\mathbf{C}(\tau_n)$, $\dot{\mathbf{C}}(\tau_n)$ and $\ddot{\mathbf{C}}(\tau_n)$ respectively. Similarly, the discretized equation (27) for the transverse vibration may be rewritten as

$$\mathbf{M}_s\mathbf{a}^s_{n+1-\alpha_m} + 2c\,\mathbf{G}_s\mathbf{v}^s_{n+1-\alpha_f} + [\mathbf{K}_{sc}(\mathbf{d}^c_{n+1-\alpha_f}) - c^2\mathbf{K}_s + \dot{c}\,\mathbf{G}_s]\,\mathbf{d}^s_{n+1-\alpha_f} = \mathbf{F}^s_{n+1-\alpha_f}, \tag{36}$$

where

$$\mathbf{d}^s_{n+1-\alpha_f} = (1-\alpha_f)\,\mathbf{d}^s_{n+1} + \alpha_f\,\mathbf{d}^s_n, \qquad \mathbf{v}^s_{n+1-\alpha_f} = (1-\alpha_f)\,\mathbf{v}^s_{n+1} + \alpha_f\,\mathbf{v}^s_n,$$

$$\mathbf{a}^s_{n+1-\alpha_m} = (1-\alpha_m)\,\mathbf{a}^s_{n+1} + \alpha_m\,\mathbf{a}^s_n, \qquad \mathbf{F}^s_{n+1-\alpha_f} = \mathbf{F}_s((1-\alpha_f)\,\tau_{n+1} + \alpha_f\,\tau_n), \tag{37}$$

$$\mathbf{d}^s_{n+1} = \mathbf{d}^s_n + \Delta\tau\mathbf{v}^s_n + (\tfrac{1}{2}-\beta)\,\Delta\tau^2\mathbf{a}^s_n + \beta\Delta\tau^2\mathbf{a}^s_{n+1}, \qquad \mathbf{v}^s_{n+1} = \mathbf{v}^s_n + (1-\gamma)\,\Delta\tau\mathbf{a}^s_n + \gamma\Delta\tau\mathbf{a}^s_{n+1}, \tag{38}$$

in which $\mathbf{d}^s_n$, $\mathbf{v}^s_n$ and $\mathbf{a}^s_n$ are approximations to $\mathbf{S}(\tau_n)$, $\dot{\mathbf{S}}(\tau_n)$ and $\ddot{\mathbf{S}}(\tau_n)$ respectively.

Although equation (36) is a non-linear coupled equation between $\mathbf{d}^s_n$ and $\mathbf{d}^c_n$, the use of a non-linear equation solver, e.g., the Newton–Rhapson method, in order to update the displacement, velocity and acceleration vectors, can be avoided. After $\mathbf{d}^c_{n+1}$, $\mathbf{v}^c_{n+1}$ and $\mathbf{a}^c_{n+1}$ are computed from equations (33)–(35) for given $\mathbf{d}^c_n$, $\mathbf{v}^c_n$ and $\mathbf{a}^c_n$, the vector $\mathbf{d}^c_{n+1-\alpha_f}$ becomes a known vector. At this time, equation (36) becomes a linear equation with a given stiffness matrix at each time step, so that the updated vector for the transverse vibration, $\mathbf{d}^s_{n+1}$, $\mathbf{v}^s_{n+1}$ and $\mathbf{a}^s_{n+1}$ can be computed from equations (36)–(38) without applying a non-linear equation solver.

The time histories of the longitudinal and transverse deflections are computed from equations (33)–(38), when the torque M_T of Figure 1(a) has a constant positive value for $0 \leqslant \tau \leqslant 50$, zero for $50 \leqslant \tau \leqslant 150$, and a constant negative value for $150 \leqslant \tau \leqslant 200$. The associated velocity profile is plotted in Figure 4, which implies that the translating acceleration $\dot{c}$ has the same pattern as M_T. When computing the time histories of the deflections, the dimensionless longitudinal load of $h = 0{\cdot}25$ and the dimensionless transverse load of the unit impulse are applied to the string. The total number of the basis functions and the time step size are selected as $J = N = 20$ and $\Delta\tau = 0{\cdot}2$.

Consider the effects of the translating acceleration on the string vibrations. The computed longitudinal and transverse deflections at $\xi = 0{\cdot}5$ are plotted with τ in Figures 5 and 6(a), when the generalized-α method has no numerical dissipation. Figures 5 and 6(a) show that the periods of the longitudinal vibration are shorter than those of the transverse vibration. This phenomenon is coincident with Figure 2, which shows that the natural frequencies of the longitudinal vibration are larger than those of the transverse vibration for the same translating speed. On the other hand, as shown in Figure 5, the longitudinal vibration has a negative average value when $0 \leqslant \tau \leqslant 50$ while it has a positive average value when $150 \leqslant \tau \leqslant 200$. This results from the inertia effect related with the acceleration. When the

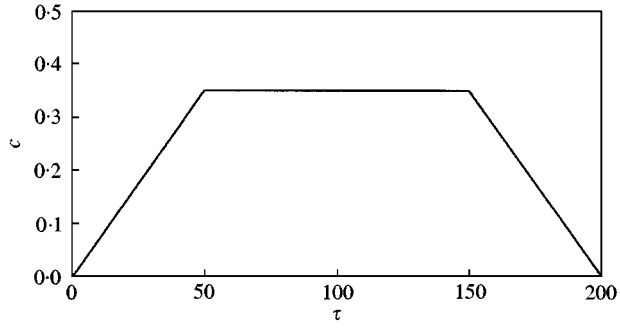

Figure 4. Time history of the dimensionless translating speed.

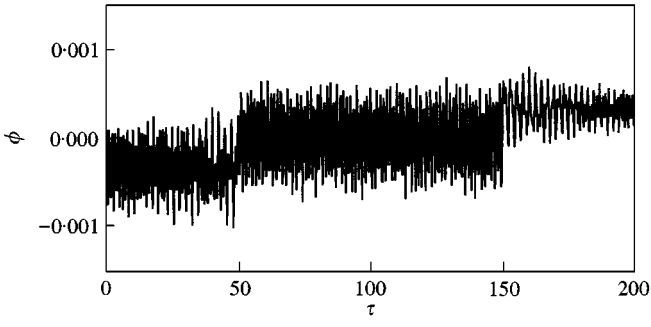

Figure 5. Time histories of the dimensionless longitudinal deflection at $\xi = 0{\cdot}5$ for the velocity profile of Figure 4 when $h = 0{\cdot}25$.

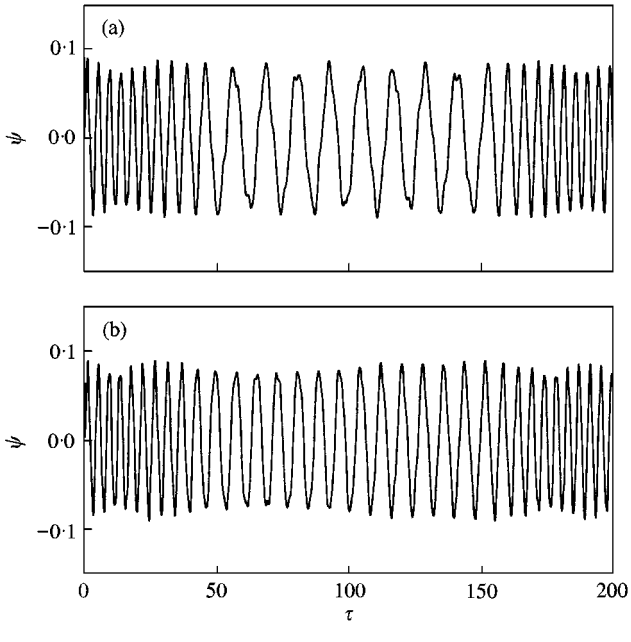

Figure 6. Comparison of the time histories for the dimensionless transverse deflection at $\xi = 0{\cdot}5$ for the velocity profile of Figure 4 when $h = 0{\cdot}25$: (a) the non-linear theory; and (b) the linear theory.

acceleration is zero, that is, $50 \leqslant \tau \leqslant 150$, it is natural that the average value of the longitudinal vibration becomes zero. Figure 6(a) illustrates that the period increases with the translating speed. This behaviour of the axially moving string with acceleration is very similar with that of the spinning disc with angular acceleration [14].

It is interesting to compare the computation results of the linear and non-linear theories. The linear theory for the transverse deflection of an axially accelerating string was introduced by Pakdemirli *et al.* [7, 8], in which the linear equation is corresponding to the linearized version of equation (27):

$$\mathbf{M}_s\ddot{\mathbf{S}} + 2c\mathbf{G}_s\dot{\mathbf{S}} + [(h - c^2)\mathbf{K}_s + \dot{c}\,\mathbf{G}_s]\,\mathbf{S} = \mathbf{F}_s. \tag{39}$$

Since the tension is uniform in the linear theory, it is not necessary to derive the linearized equation of motion for the longitudinal deflection. With the same conditions in the above, the time history for the transverse deflection at $\xi = 0{\cdot}5$ is computed from the linear equation

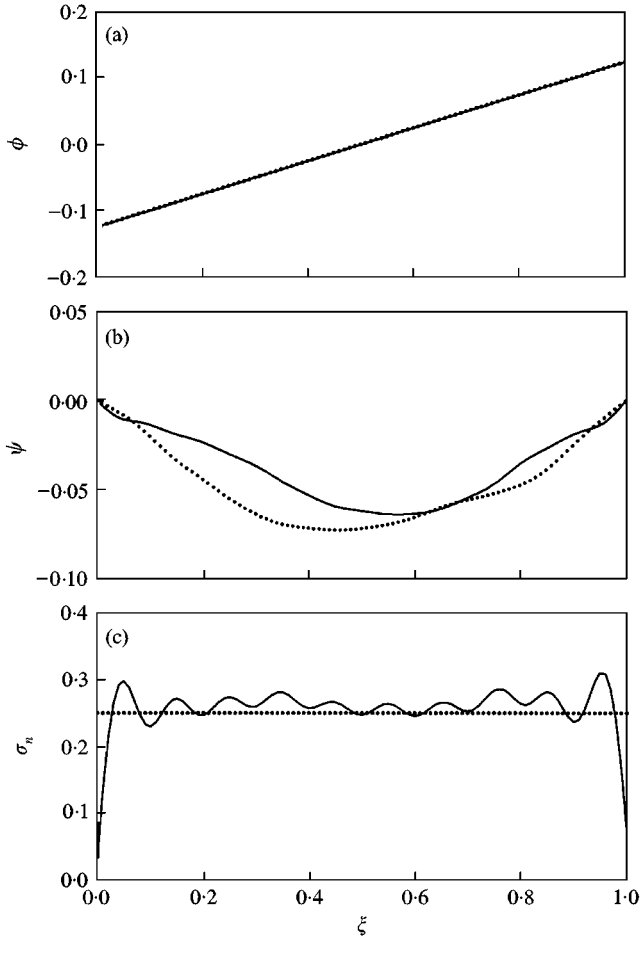

Figure 7. Comparison of the deflection and stress distributions between the non-linear theory (——) and the linear theory (·····) when $h = 0{\cdot}25$, $\tau = 20$, $c = 0{\cdot}14$ and $\dot{c} = 0{\cdot}07$: (a) the dimensionless longitudinal deflection; (b) the dimensionless transverse deflection; and (c) the dimensionless stress.

of motion given by equation (39). Figure 6(a) represents the time response from the non-linear theory while Figure 6(b) represents the time response from the linear theory. It is noted in Figure 6 that the response of the non-linear theory is quite different from that of the linear theory, that is, the period of Figure 6(a) is longer than that of Figure 6(b).

Finally, it is valuable to investigate what difference the linear and non-linear theories yield in the deflection and stress distributions along the string. The distributions are computed and presented in Figure 7, when $h = 0{\cdot}25$ and $\tau = 20$. The dimensionless time of $\tau = 20$ corresponds to $c = 0{\cdot}14$ and $0{\cdot}07$ in Figure 4. The dotted and solid lines stand for the distributions from the linear and non-linear theories respectively. As shown in Figure 7(a), it is hard to find a difference between the longitudinal deflection distributions from the linear and non-linear theories. However, Figure 7(b) demonstrates that the transverse deflection distribution of the non-linear theory has a large difference from the distribution of the linear theory. As is well known, in the linear theory, the stress is constant because the tension is uniform along the string. On the other hand, the stress is not constant in the non-linear theory. The stress of the non-linear theory may be measured by the dimensionless stress defined as

$$\sigma_n = \frac{\partial \phi}{\partial \xi} + \frac{1}{2}\left(\frac{\partial \psi}{\partial \xi}\right)^2. \tag{40}$$

The stress distributions in Figure 7(c) show that the stress from the linear theory is uniform along the string while the stress from the non-linear theory fluctuates. In Figure 7(c), the value corresponding to the dotted line is the averaged value of the solid line. This value is the slope of the dotted line in Figure 7(a), which is represented by the first term on the right-hand side of equation (40). Therefore, the fluctuation originates from the geometric non-linearity that is represented by the second term on the right-hand side of equation (40).

6. CONCLUSIONS

The equations of motion for the axially moving string are derived, simultaneously considering the longitudinal and transverse deflections, the geometric non-linearity and the translating acceleration. The derived equations consist of a linear equation for the longitudinal vibration and a non-linear equation for the transverse equation. Especially, the non-linear equation is a coupled equation between the transverse and longitudinal deflections. Applying the Galerkin method to the equations of motion results in the discretized equations, in which the natural frequencies and time responses are computed.

From the computation of the natural frequencies, the effects of the translating speed and the longitudinal load are examined for the longitudinal and transverse vibrations. The time histories for the deflections the distributions for the deflections and stresses are computed by using the generalized-α time integration method. The results of this study are summarized as follows.

(1) The critical speeds are $c = 1$ and $\sqrt{h}$ for the longitudinal and transverse vibrations respectively.
(2) The natural frequencies for the longitudinal vibration are independent of h while the frequencies for the transverse vibration are dependent on h.
(3) The longitudinal vibration has negative, zero and positive average values for the positive, zero and negative accelerations respectively.
(4) The period of the transverse vibration increases with the translating speed.

(5) The transverse response of the non-linear theory is quite different from that of the linear theory.
(6) The stress from the linear theory is uniform along the string while the stress from the non-linear theory fluctuates.

ACKNOWLEDGMENT

This study was supported by the Brain Korea 21 Project of the Ministry of Education, Republic of Korea. This support is gratefully acknowledged.

REFERENCES

1. C. D. MOTE JR. 1972 *Shock and Vibration Digest* **4**, 2–11. Dynamic stability of axially moving materials.
2. J. A. WICKERT and C. D. MOTE JR. 1988 *Shock and Vibration Digest* **20**, 3–13. Current research on the vibration and stability of axially moving materials.
3. C. D. MOTE JR. 1966 *Journal of Applied Mechanics* **33**, 463–464. On the nonlinear oscillation of an axially moving string.
4. A. L. THURMAN and C. D. MOTE JR. 1969 *Journal of Applied Mechanics* **36**, 83–91. Free, periodic, non-linear oscillation of an axially moving string.
5. Y. C. FUNG 1977 *A First Course in Continuum Mechanics*. Englewood Cliffs, NJ: Prentice-Hall, Inc.
6. C. D. MOTE JR. 1975 *Journal of Dynamic Systems, Measurements and Control* **97**, 96–98. Stability of systems transporting accelerating axially moving materials.
7. M. PAKDEMIRLI, A. G. ULSOY and A. CERANOGLU 1994 *Journal of Sound and Vibration* **169**, 179–196. Transverse vibration of an axially accelerating string.
8. M. PAKDEMIRLI and A. G. ULSOY 1997 *Journal of Sound and Vibration* **203**, 815–832. Stability of an axially accelerating string.
9. E. OZKAYA and M. PAKDEMIRLI 2000 *Journal of Sound and Vibration* **230**, 729-742. Lie group theory and analytical solutions for the axially accelerating string problem.
10. D. B. MCIVER 1972 *Journal of Engineering Mathematics* **7**, 249–261. Hamilton's principle for systems of changing mass.
11. J. CHUNG and G. M. HULBERT 1993 *Journal of Applied Mechanics* **60**, 371–375. A time integration algorithm for structural dynamics with improved numerical dissipation: the generalized-α method.
12. M. A. CRISFIELD 1991 *Non-linear Finite Element Analysis of Solids and Structures*. Chichester: John Wiley and Sons.
13. T. J. R. HUGHES 1987 *The Finite Element Method*. Englewood Cliffs, NJ: Prentice-Hall, Inc.
14. J. CHUNG, J.-E. OH and H. H. YOO 2000 *Journal of Sound and Vibration* **231**, 375–391. Non-linear vibration of a flexible spinning disc with angular acceleration.